JEE Journal of Ecological Engineering

Journal of Ecological Engineering 2022, 23(5), 293–304
https://doi.org/10.12911/22998993/147318
ISSN 2299–8993, License CC-BY 4.0

Received: 2022.02.21
Accepted: 2022.03.19
Published: 2022.03.29

Ability of Response Surface Methodology to Optimize Photocatalytic Degradation of Amoxicillin from Aqueous Solutions Using Immobilized TiO_2/Sand

Fadia A. Sulaiman[1*], Abeer I. Alwared[2]

[1] Water Resource Technical, Al-Hawija Technical Institute, Iraq
[2] Department of Environmental Engineering/ College of Engineering, University of Baghdad, Iraq
* Corresponding author's e-mail: f.sulaiman0911@coeng.uobaghdad.edu.iq

ABSTRACT

The response surface method was applied to optimize operational factors in the solar photocatalytic process on the removal of Amoxicillin (AMOX) residues from aqueous solution using TiO_2 immobilized on the sand as a catalyst. The results reveal that the degradation percentage of AMOX is 93.12%, when optimal conditions of pH=5, 75 mg/l of TiO_2, 400 mg/l of H_2O_2, and 10 mg/l of AMOX concentration at 150 min irradiation time were used. Furthermore, the model's expected response results have reasonable similarity with the actual data (R^2 = 93.58%), demonstrating the efficiency of this method in making an accurate prediction. A second-order polynomial multiple regression model was used to evaluate the responses, which confirms that was a satisfactory adjustment with the achieved data through analysis of variance (R^2 = 93.58%, R^2_{adj} = 91.48% and R^2_{pred} =89.68%). In addition, it is observed that the removal of undesirable compounds follows a pseudo-2nd order kinetic model with R^2 = 0.9862. In conclusion, with the ease of usage of immobilized TiO_2 and good photocatalytic efficiency, the findings showed the potential application to the antibiotics from an aqueous solution.

Keywords: amoxicillin; solar photocatalyst; immobilized TiO_2; sand; RSM; kinetics.

INTRODUCTION

Pharmaceutical products are one of the most serious and concerning environmental issues since they tend to survive in the environment for longer periods of time due to their recalcitrance and ultra-low biodegradability (Tarfiei et al., 2018; Chauhan et al., 2018). Amoxicillin, ciprofloxacin, and tetracycline are the widest drugs used in the world for the treatment of a variety of bacterial illnesses (Mohammed et al., 2020a). Numerous conventional wastewater treatment techniques for removing pharmaceutical residues have been reported. Unfortunately, most standard treatments have failed to entirely remove pharmaceutical chemicals from water, necessitating the development of new technologies to remove pharmaceutical compounds from aquatic sources (Chauhan et al., 2018). AOPs (advanced oxidative processes) may provide a solution to this problem. They allow contaminants to be degraded by highly oxidizing species formed in the reaction media, such as hydroxyl radicals. Heterogeneous photocatalysis with TiO_2 as a photocatalyst looks to be the most promising destructive technology among AOPs. At ambient temperature and pressure, photocatalysis has gained traction as a viable approach for the destruction of persistent organic pollutants (Mohammed et al., 2020b).

Photocatalysts are substances that destroy the contaminants of water and wastewater, and convert them into harmless substances such as water and carbon dioxide. Photocatalyst is a substance that can induce a chemical reaction by the light exposure while it would not be subject to any changes. Among the substances most widely used for photocatalysis are the Titanium dioxide (TiO_2)-based compounds used in water and wastewater treatment (Chen et

al., 2017), also it is cheap and non-toxic and having high and stable photoactivity (Bielan et al., 2020). Photoreactors used in heterogeneous photocatalysis can be divided into two types: slurry reactors with suspended catalyst particles and reactors with catalyst immobilized on various inert substrates. In comparison to reactors with immobilized catalyst, slurry reactors have a large surface area for reactions, allowing for faster pollutant degradation. Particle aggregation at high photocatalyst concentrations, the need for a filtration step after the photocatalytic treatment, and the inability to use a continuous process are all disadvantages of reactors with suspended catalyst (Manassero et al., 2017). Chemical spray pyrolysis, hydrothermal synthesis, electrodeposition, chemical vapor deposition, atomic layer deposition and sol-gel are the most widely used preparation methods for immobilized catalyst: (Méndez-López et al., 2020). The sol-gel method offers a simple and convenient pathway for the synthesis of advanced material systems and for applying them as surface coatings. A large verity of surfaces has been used by authors to support catalyst, such as stainless steel (Danfá et al., 2021), glass slides (Morjène et al, 2020), glass spheres (Kutuzova et al, 2021) beads (Sharma et al., 2020), and Raschig rings (Tong et al., 2020), zeolites (Ngoepe et al., 2020). The response surface methodology (RSM) is a set of mathematical and statistical techniques focused on fitting a polynomial equation to experimental data in order to forecast a system's behavior and save time and money as operating conditions change (Dutta, 2015). The traditional optimization strategy involves changing one variable at a time while keeping the other parameters fixed. The traditional method, on the other hand, is incapable of determining the intricate interaction between variables and responses (Darvishmotevalli et al., 2019).

There are many methods to optimize the processes such as Box Behnken Design (BBD), and Face centered design (FCD) and central composite design (CCD). Among of these methods the CCD was widely applied, due to its simple structure and good efficiency. The goal of this research is to determine the performance of TiO_2 supported on sand/ hydrogen peroxide /sun radiation for the removal of AMOX residue from synthetic wastewater based on pH, irradiation time, initial concentration of AMOX, hydrogen peroxide concentration and titanium dioxide. In addition, CCD was utilized to create mathematical equations for pollutant elimination, allowing for a quantitative assessment of the AOP process employed to degrade AMOX. The diagnostic checking tests offered by analysis of variance are then used to determine the adequacy of the proposed model.

MATERIAL AND METHOD

Materials

Amoxicillin powdered was chosen as contaminant model with purity 99% without further purification gotten from the general company for drugs industry (Iraq) (original manufacturer: Merch, Germany). Their chemical structure and specification was shown in Figure 1 and Table 1, respectively. Titanium tetra-isopropoxide (TTIP) contained 95% anatase and 5% rutile and Isopropanol have been used for support TiO_2. Hydrogen peroxide H_2O_2 (50% w/w) obtained from Merck was used as an oxidizing agents. The pH value of the aqueous solution was adjusted using HCl and/or NaOH. However, because of its high density (specific gravity 2.65), local availability, low cost, chemical inertness, mechanical resistance, and abundance in varied particle sizes, natural sand of zone (1) complying to IQS No.45/1984 was utilized to support TiO_2.

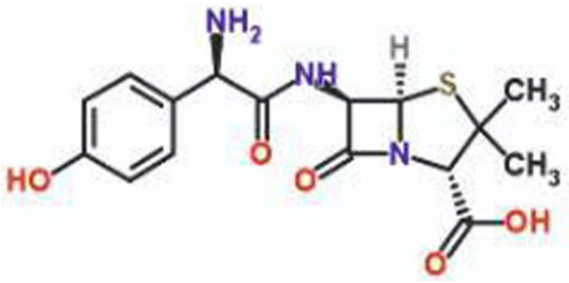

Fig. 1. Chemical structure of AMOX

Table 1. Main properties of the Amoxicillin (Balarak et al., 2017)

Parameter	Character/value
Molecular formula	$C_{16}H_{19}N_3O_5S$
Molar mass	365.4 g/mol
Solubility in water	3430 mg/L at 20 °C
Dissociation constant (pKa)	2.4 (carboxyl), 7.4 (amine), and 9.6 (phenol)
Henry's law constant	2.73 x 10^{-19} at 20 °C

Experimental work and analysis

TiO2 immobilization

Sol-gel dip-coating technique was used for direct immobilization of TiO_2 on sand (TiO_2/sand). Firstly, sand was washed thoroughly with tap water and then distilled water after that dried at 120°C for 2 hours to remove organic impurities. The dried sand was sieved to obtain grain sizes ranging from 150–180 microns and kept in polyethylene bags for further use. The desired molar ratio of TTIP: isopropanol: water (1:25:10, 2:25:10, 3:25:10, 5:25:10) was stirred by using magnetic stirrer and then sand was added. Furthermore the coated sand was dried in a muffle furnace at 120°C for 2 hours, after that leave it in the furnace for one hour at 500°C and, then leave to cool. The thickness of the immobilized TiO2 film was then increased with a second coating cycle. Finally, unconnected TiO2 particles were removed by washing covered sand with distilled water (Abdel-Maksoud et al., 2018), and kept for further use (Fig. 2).

Procedure and analysis

Photocatalytic degradation process was carried out in a batch mode reactor under solar irradiation (Fig. 3). The reactor consisted of Pyrex glass (1L) painted by silver nitrate to act as excellent reflective for solar power (Zaier et al., 2017) and contained a piece of mirror at the bottom (used as reflector). Different concentrations of AMOX solution (10, 30, 50, 80 and 100) mg/L were prepared then pH was adjusted, (using pH meter type INOLAB 72, WTW Co., Weilheim, Germany) by adding a dilute solution of HCl or NaOH to the reactor contents and at room temperature. Where after the desired concentration of TiO_2/sand (50, 75, 100) mg/L was added to the solution. The suspension was magnetically stirred

Fig. 2. TiO_2 immobilized on sand

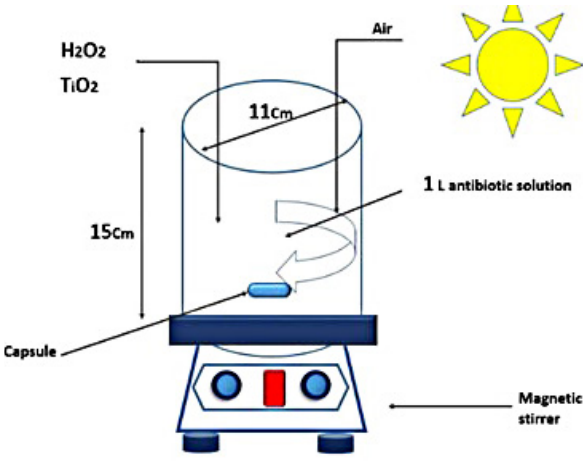

Fig. 3. Schematic diagram of the batch reactor

using a magnetic stirrer type (MSH-300N, BOECO, Hamburg, Germany) at 200 rpm for 150 min. To achieve primary adsorption equilibrium, first spend 30 minutes in the dark between AMOX and TiO_2/sand, subsequently H_2O_2 (250, 400, 600 and 800) mg/L was added and then switching on the lamp to start the reaction. To separate the catalyst, 10 ml of the sample was extracted and centrifuged at 200 rpm for 15 minutes at regular intervals. The concentration of AMOX in each sample was measured at 278 nm using a spectrophotometer (UV-Vis Spectrophotometer Perkin–Elmer 55 OSE). However, the following equation was used to compute the target compound's elimination efficiency:

$$\text{Removal percentage} = \frac{C_o - C_e}{C_o} \times 100 \quad (1)$$

where: *Co* and *Ce* represent the primary and equilibrium drug concentration (mg/l), respectively.

RESPONSE SURFACE DESIGN

The DOE software serves as a foundation for the creation of experimental runs. The Central Composite Design (CCD) was selected in this study since it is the most typically used with DOE. The effects of AMOX concentration, TiO_2/sand dosage, H_2O_2 concentration, pH, and time were studied using CCD. Table 2 shows the number of variables and their ranges, which were determined using linked scientific literature as well as experimental data obtained in preliminary study utilizing the AMOX antibiotic. The variables were analyzed at two levels: (minimum) and (maximum), using the whole face-centered

Table 2. Experimental range and levels of the independent variables

Factor	Name	Unit	Lower limit	Upper limit	Lower weight	Upper weight	Importance
A	AMOX conc.	Mg/L	10	100	1	1	3
B	TiO_2 conc.	Mg/L	50	200	1	1	3
C	H_2O_2 conc.	Mg/L	200	800	1	1	3
D	pH	--	3	11	1	1	3
E	Time	Min	30	150	1	1	3
R	Removal	%	7.82	93.12	1	1	3

CCD experimental plan as a guide. RSM was used to create mathematical models for photocatalytic reactors in the form of multiple regression equations. All conceivable factor combinations' main and interaction effects have been calculated. A third-order polynomial equation was utilized to fit the experimental data in Eq. 2 for the creation of regression equations relating to the corrosion process (Salam et al., 2015):

$$\begin{aligned} Y = {} & \beta_o + \beta_A A + \beta_B B + \beta_C C + \beta_D D + \\ & \beta_{AA}A^2 + \beta_{BB}B^2 + \beta_{CC}C^2 + \beta_{DD}D^2 + \\ & \beta_{AB}AB + \beta_{AC}AC + \beta_{AD}AD + \beta_{BC}BC + \\ & \beta_{BD}BD + \beta_{CD}CD + \beta_{AAA}A^3 + \beta_{BBB}B^3 + \\ & \beta_{CCC}C^3 + \beta_{DDD}D^3 + \beta_{AAB}A^2B + \beta_{AAC}A^2C + \\ & \beta_{AAD}A^2D + \beta_{ABB}AB^2 + \beta_{ACC}AC^2 + \\ & \beta_{ADD}AD^2 + \beta_{ABB}AB^2 + \beta_{BBC}B^2C + \\ & \beta_{BBD}B^2D + \beta_{BCC}BC^2 + \beta_{BDD}BD^2 + \\ & \beta_{CDD}C^2D + \beta_{CDD}CD^2 + \beta_{ABC}ABC + \\ & \beta_{ABD}ABD + \beta_{ACD}ACD + \beta_{BCD}BCD \end{aligned} \quad (2)$$

where: β_o – offset term,
$\beta_A, \beta_B, \beta_C, \beta_D$ – linear effect terms,
$\beta_{AA}, \beta_{BB}, \beta_{CC}, \beta_{DD}$ – squared effects,
$\beta_{AB}, \beta_{AC}, \beta_{AD}, \beta_{BC}, \beta_{BD}, \beta_{CD}, \beta_{AAB}, \beta_{AAC}, \beta_{AAD}, \beta_{ABB}, \beta_{ACC}, \beta_{ADD}, \beta_{ABB}, \beta_{BBC}$ – interaction,
$\beta_{BBD}, \beta_{BCC}, \beta_{BDD}, \beta_{CDD}, \beta_{ABC}, \beta_{ABD}, \beta_{ACD}, \beta_{BCD}$ – effects,
$\beta_{AAA}, \beta_{BBB}, \beta_{CCC}, \beta_{DDD}$ – cubed effects
Y – fitted response.

Model terms are chosen or ignored based on the probability of error (P) value with a confidence level of 0.95. An analysis of variance was used to examine the statistical results produced using CCD (ANOVA). Design expert software was used to analyze the data, create the experimental design, and optimize the interaction effect of independent factors on the answer.

RESULTS AND DISCUSSIONS

Optimization representation

The results of experiments in the form of removal percentage of AMOX from aqueous solution were appraised based on the CCD were shown in Table 3. The use of RSM's historical data design yielded a regression model for the response of corrosion rate, which suggested fitting the response data with a third-order polynomial model (Salam et al., 2015). The model is a modified cubic model that was generated through manual reduction and simplification of the model, which included deleting bigger inconsequential elements to get the final empirical model in terms of actual factors, as shown in Eq. 3:

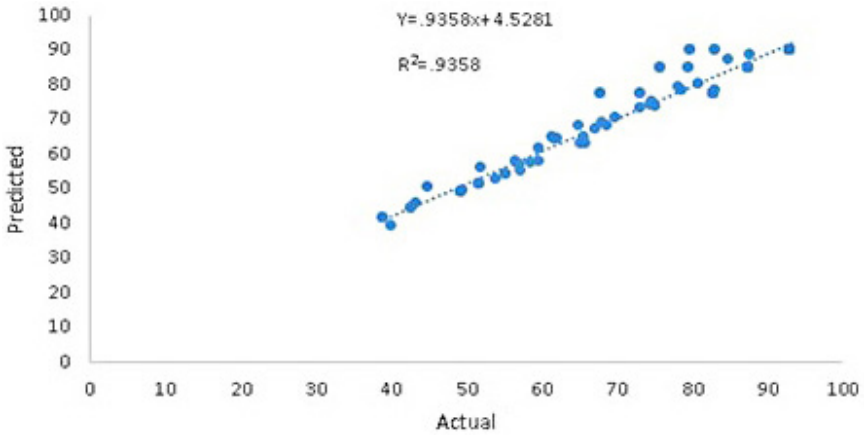

Fig. 4. Relation between predicted and actual data of AMOX removal

Table 3. Results of experiments according to CCD

Run	pH	Time	AMOX conc.	TiO_2 /sand amount	H_2O_2 conc.
1	8	82.5	55	125	500
2	5	15	10	200	800
3	5	15	100	200	200
4	11	15	100	200	800
5	11	15	100	50	800
6	11	15	100	200	200
7	11	150	10	200	800
8	5	150	100	200	200
9	11	150	10	50	200
10	11	150	10	50	800
11	5	150	100	50	800
12	8	82.5	55	125	500
13	8	-78.043	55	125	500
14	11	15	10	50	800
15	5	150	10	200	800
16	11	150	100	200	200
17	11	150	100	50	800
18	5	15	100	50	200
19	11	150	100	50	200
20	8	82.5	55	125	500
21	5	150	10	50	800
22	5	150	10	200	200
23	8	82.5	-52.0286	125	500
24	8	82.5	55	125	1213.524
25	5	150	100	50	200
26	11	15	10	50	200
27	11	150	10	200	200
28	5	15	10	200	200
29	11	150	100	200	800
30	8	243.043	55	125	500
31	5	15	100	200	800
32	5	150	10	50	200
33	8	82.5	55	125	-213.524
34	11	15	10	200	800
35	5	15	10	50	200
36	11	15	100	50	200
37	8	82.5	162.0286	125	500
38	8	82.5	55	-53.3811	500
39	8	82.5	55	125	500
40	8	82.5	55	125	500
41	0.864757	82.5	55	125	500
42	5	150	100	200	800
43	5	15	10	50	800
44	15.13524	82.5	55	125	500
45	11	15	10	200	200
46	5	15	100	50	800
47	8	82.5	55	303.3811	500

$$AMOX\ removal = -699.56812 - 1.27630A + 11.81151B + 1.46411C + 96.00149D + 1.37018E + 0.006388AE - 0.006685CE + 0.018603A^2 - 0.121647B^2 - 0.003136C^2 - 14.20631D^2 - 0.001623E^2 - 0.000060A^2E + 0.000015C^2E - 0.000106A^3 + 0.000352B^3 + 1.97945\text{E} - 06C^3 + 0.635221D^3 - 9.35199\text{E} - 09C^3E \quad (3)$$

The predicted and actual AMOX removal percentage was given in Figure 4. According to the results the points given in this scheme have reasonable correlations. With respect to the equation addressed here, as the antibiotic concentration was increased, the removal reduced progressively with increasing units of contact time, and as the catalyst dose was increased, the removal increased, and the model properly explained the experimental range tested.

Variance analysis (ANOVA)

The results achieved from the ANOVA analysis (Table 4) demonstrated that R^2, adjusted R^2 (R^2_{adj}) and predicted R^2 (R^2_{pred}) for the removal of AMOX were 0.9358, 0.9148 and 0.8968, respectively. The correlation coefficients. and were found to be close to each other, This suggests that the regression model explains the connection between the independent variables and the response very well. The *P*-value and *F*-value used for response were used to determine the relevance of the model term. A bigger *F*-value and a smaller amount of probability signified a stronger relevance of the associated model in this study. The probability value (0.0001) was determined to be quite low, indicating that the term was significant for the model. With respect to the equation addressed here, as the antibiotic concentration was increased, the removal reduced progressively with increasing units of contact time, and as the catalyst dose was increased, the removal increased, and the model properly explained the experimental range tested. (Ozturk et al., 2017). In addition Table 5 shows Adeq Precision ratio was 21.734% which means an adequate signal. In which Adeq Precision measures the ratio of signal to noise, and is desirable at a ratio > 4 (Darvishmotevalli et al., 2019).

Response surface and contour plots for AMOX residue removal

The model-predicted response's three-dimensional (3D) response surface and two-dimensional (2D) contour plot for solar photocatalytic removal of AMOX removal from aqueous solutions.

Initial value of pH

The effect of different initial pH value (3, 5, 7 and 11) on AMOX removal was studied while keeping other parameters constant (AMOX conc. = 10 mg/l, H_2O_2 = 400 mg/l, and TiO_2 = 75 mg/l), and their results were plotted in Figure 5, as can be seen in this figure, that the removal efficiency of AMOX decreased at low and high pH value due to the ionization states of the substrate and the catalyst where that AMOX is positively charged at acidic pH while at alkaline pH it is negatively charged. On the other hand TiO_2 surface charge change from positive to negative. Point zero charge for TiO_2 was 6.8 (Tio, 2017). Where the pH affects the electrostatic load of the TiO_2 surface at photocatalytic reactions.TiO_2 particles are shown to be granule in an aqueous medium due to the pH and ionic strength. It is known that agglomeration of TiO_2 particles is lower at acidic conditions than at alkaline ones (Türkay and Kumbur, 2019). The increase in degradation rate when pH rises from 3 to 5 is due to more extensive hydroxyl radical production at higher pH on the one hand, and antibiotic hydrolysis on the other. Because AMOX and TiO_2 have the same charge (negative) at alkaline pH as they do at acidic pH, adsorption is hindered once more (Tio, 2017). Therefore, the best removal was achieved at pH 5 and this results were in agreement with finding of (Elmolla et al, 2010; Kalash and Al-Furaiji, 2020; Malakootian et al, 2019)

Initial concentration of AMOX and reaction time

The effect of the initial concentration of AMOX on the photocatalytic efficiency was investigated with concentrations ranging from 10 to 100 mg/l, immobilization TiO_2 = 75 mg/l, H_2O_2 = 400 mg/l, and pH = 5 and their results were plotted in Figure 6. According to this graph, when the starting AMOX concentration increased from 10

Table 4. The results of the analysis of variance for the response quadratic models

Std. Dev.	Mean	C V %	R^2	R^2_{adj}	R^2_{pred}	Adeq Precision
4.6	70.49	6.53	0.9358	0.9148	0.8968	21.734

Table 5. The ANOVA results for the design expert software equation

Source	Sum of Squares	df	Mean Square	F-value	p-value	Significance
Model	17891.12	19	941.64	44.49	< 0.0001	significant
A-conc. Amox(mg/l)	84.11	1	84.11	3.97	0.0509	
B-conc.TiO2(mg/l)	6436.30	1	6436.30	304.09	< 0.0001	
C-conc.H2O2(mg/l)	1041.14	1	1041.14	49.19	< 0.0001	
D-PH	881.75	1	881.75	41.66	< 0.0001	
E-Time	584.27	1	584.27	27.60	< 0.0001	
AE	2.39	1	2.39	0.1131	0.7378	
CE	84.48	1	84.48	3.99	0.0504	
A^2	233.35	1	233.35	11.03	0.0016	
B^2	3537.87	1	3537.87	167.15	< 0.0001	
C^2	347.68	1	347.68	16.43	0.0002	
D^2	384.57	1	384.57	18.17	< 0.0001	
E^2	142.61	1	142.61	6.74	0.0119	
A^2E	75.41	1	75.41	3.56	0.0641	
C^2E	8.48	1	8.48	0.4007	0.5292	
A^3	71.64	1	71.64	3.38	0.0709	
B^3	4933.68	1	4933.68	233.10	< 0.0001	
C^3	708.15	1	708.15	33.46	< 0.0001	
D^3	861.41	1	861.41	40.70	< 0.0001	
C^3E	73.79	1	73.79	3.49	0.0669	
Residual	1227.60	58	21.17			
Lack of Fit	192.13	22	8.73	0.3036	0.9978	not significant
Pure Error	1035.48	36	28.76			
Cor Total	19118.73	77				

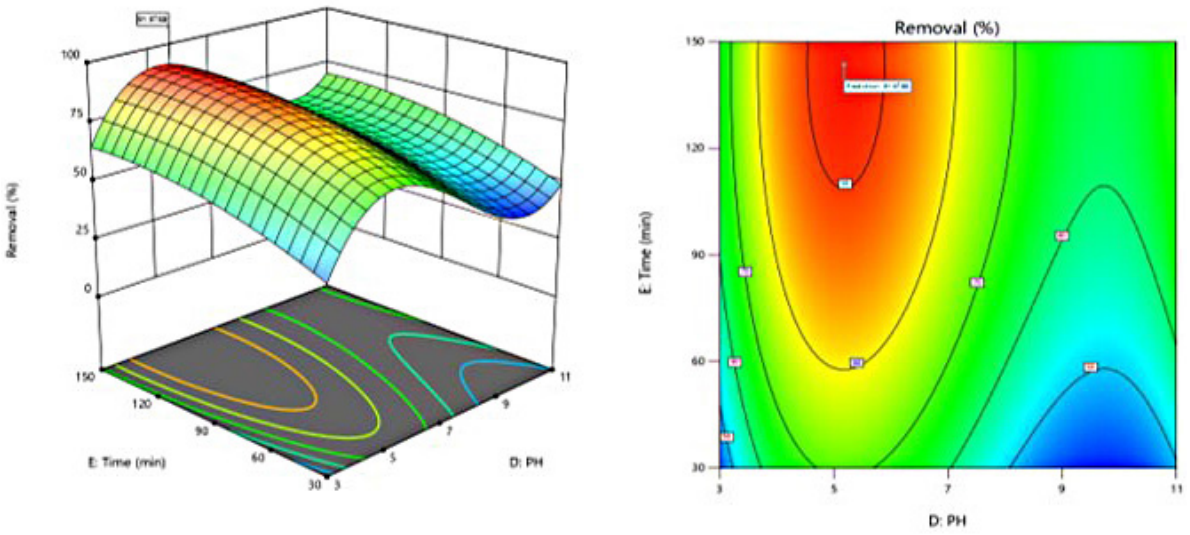

Fig. 5. 2D contour plots express and 3D surface plot of pH on removal efficiency

to 100 mg/l in the photocatalytic process, the efficiencies of AMOX degradation elimination gradually declined. The amount of antibiotic adsorbed to the photocatalyst surface increases as the antibiotic concentration rises. However, the photoactive patches on the catalyst surface are reduced, and the rate of antibiotic degradation is reduced as a result (Türkay and Kumbur, 2019). Furthermore, the concentrations of generated radicals were consistent across all samples. Lower concentrations of amoxicillin with the same quantity of hydroxyl radicals had a better chance of being

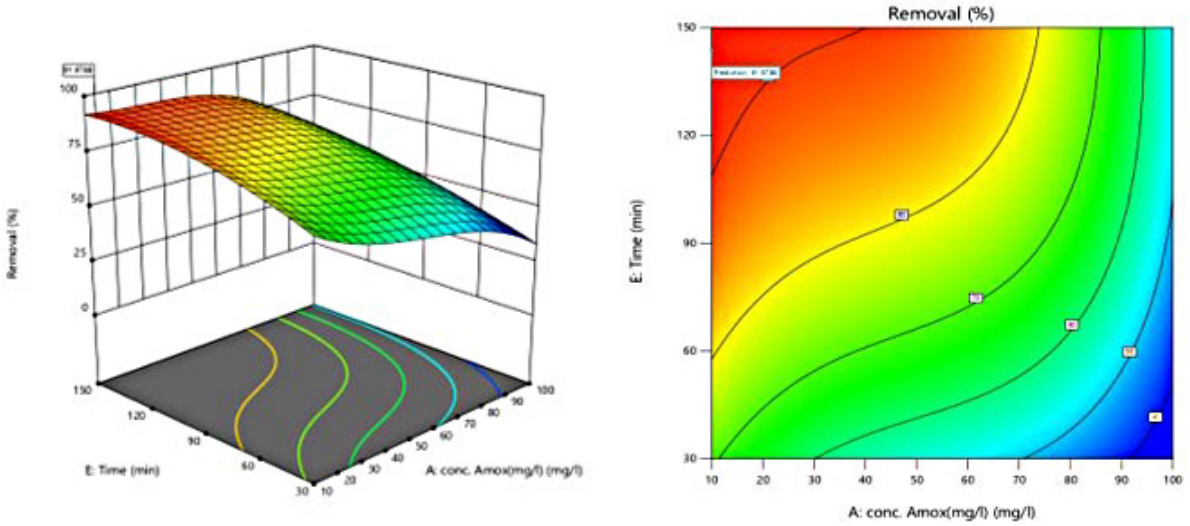

Fig. 6. 2D contour plots express and 3D surface plot of AMOX concentration on removal efficiency

removed than samples with a higher concentration of antibiotic (Olama et al, 2018; Jouali et al, 2020). According to this graph, when the starting AMOX concentration increased from 10 to 100 mg/l in the photocatalytic process, the efficiencies of AMOX degradation elimination gradually declined. The amount of antibiotic adsorbed to the photocatalyst surface increases as the antibiotic concentration rises. However, the photoactive patches on the catalyst surface are reduced, and the rate of antibiotic degradation is reduced as a result (Türkay and Kumbur, 2019).

Effect of the amount of TiO_2/sand

The effect of different amount of TiO_2/sand (50, 75, 150 and 200) mg/l on AMOX removal was studied while keeping other parameters constant (10 mg/l AMOX concentration, H_2O_2 400 mg/l, and pH 5) and plotted in Figure 7. According to this figure the degradation of AMOX increased by increasing TiO_2 concentration till it reached 75 mg/l, then it decreased until it reached 150 mg/l. Antibiotic degradation did not improve significantly when TiO_2 concentrations were raised over 150 mg/l. This could be attributed to a decrease in light penetration, increased light scattering, or aggregation of TiO_2/sand. (Olama et al., 2018). Based on the results, the optimum TiO_2/sand concentration for degradation of AMOX in aqueous solution was 75 mg/l. The reason for a decrease in the mineralization rate at high concentration of TiO_2/sand was the aggregation of TiO_2 nanoparticles at high concentrations causing a decrease in the number of surface active sites and an increase

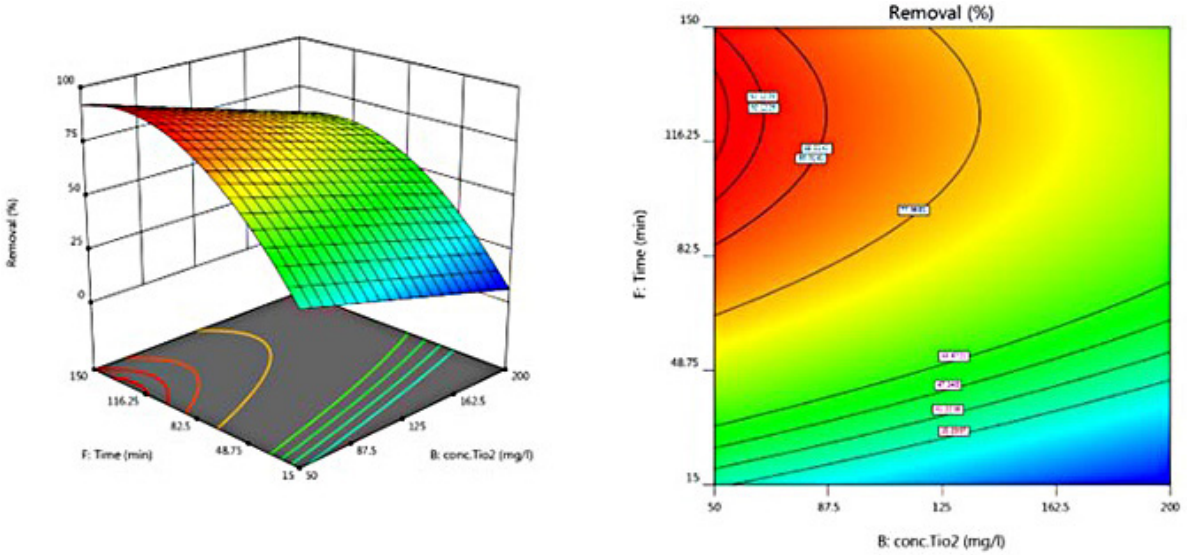

Fig. 7. 2D contour plots express and 3D surface plot of TiO_2/sand amount on removal efficiency

in the opacity and light scattering of TiO_2 nanoparticles at high concentration. This tends to reduce the amount of irradiation that passes through the sample (Olama et al., 2018). The following steps can be used to describe how UV light activates TiO_2 (Elmolla and Chaudhuri, 2010):

$$TiO_2 + hv \rightarrow TiO_2(e^- + h^+) \quad (4)$$

$$h^+ + H_2O \rightarrow H^+ + {}^*OH \quad (5)$$

$$h^+ + OH^- \rightarrow {}^*OH \quad (6)$$

$$\text{Organics} + {}^*OH \rightarrow \text{Degradation Products} \quad (7)$$

$$e- + O_2 \rightarrow {}^*O_2^- \quad (8)$$

$$H_2O_2 + e^- \rightarrow {}^*OH + OH^- \quad (9)$$

H_2O_2 concentrations

The effect of different H_2O_2 concentrations (200, 400, 600 and 800) mg/L on AMOX removal was studied, while keeping other parameters constant (AMOX concentration of 10 mg/L, pH 5, and TiO_2/sand = 75 mg/L) and their results were plotted in Figure 8.This figure reveals that the removal efficiency increased from 80.96 to 93.12% by increasing the H_2O_2 concentration from 200 to 400 mg/l, respectively. The degradation efficiency decreased as the H_2O_2 concentration increased; these irregular fluctuations might be explained by the probable scavenging action of H_2O_2, a well-known phenomena for H_2O_2 involving AOPs. A local excess of H_2O_2 caused this reaction, which resulted in the creation of $HO_2^{\bullet}$ (hydroxyperoxyl) radicals, which have a very low oxidation potential (Tekin et al., 2018) according to Eqs. 10 and 14 (Daneshvar et al., 2005; Lofrano et al., 2017):

$$TiO_2(e^-) + H_2O_2 \rightarrow TiO_2 + OH^- + {}^{\bullet}OH \quad (10)$$

$${}^{\bullet}O^{-2} + H_2O_2 \rightarrow OH^- + {}^{\bullet}OH + O_2 \quad (11)$$

$$H_2O_2 + h_v \rightarrow 2OH \quad (12)$$

$$H_2O_2 + {}^{\bullet}OH \rightarrow HO_2^{\bullet} + H_2O \quad (13)$$

$$HO_2^{\bullet} + {}^{\bullet}OH \rightarrow H_2O + O_2 \quad (14)$$

Process optimization

The optimal values of independent parameters including pH, TiO_2/sand loading, H_2O_2 concentration, and reaction time to obtain maximum removal of AMOX residue from aqueous solution using the photocatalysis process. A desirability function is created by combining the goals. Desirability is an objective function with a value of one at the goal and 0 outside of the bounds. The program looks into how to improve this feature. This functionality is being investigated by the application. The goal-finding process starts at a random location and progresses up the steepest slope to the highest peak (Ghorbani and Kamari, 2017). Figure 9, shows the desirability profile of the projected response, which shows that the values of optimal circumstances for independent variables are as follows: (pH = 5.177, TiO_2 = 69.555 mg/l, H_2O_2 = 353.254 mg/l, time= 143.568 min, and 10.0001 mg/l of AMOX concentration), under these conditions the predicted value (91.9788%) which was very adjacent to the experimentally observed value of (93.12%).

KINETIC

The kinetic model of the pseudo first order reaction (Eq. 15) and pseudo second order (Eq. 16)were used for studying 10 mg/l of AMOX

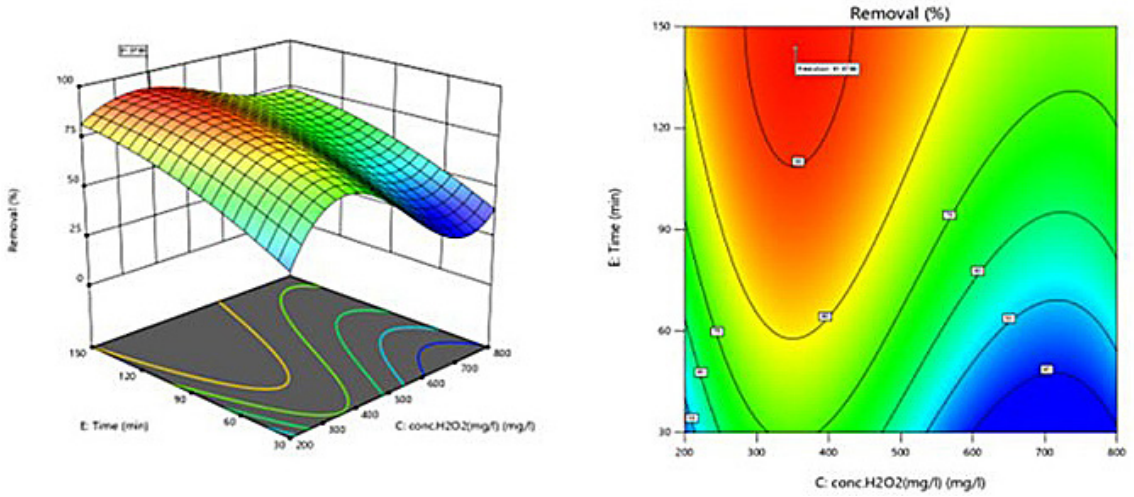

Fig. 8. Effect of H_2O_2 on AMOX degradation

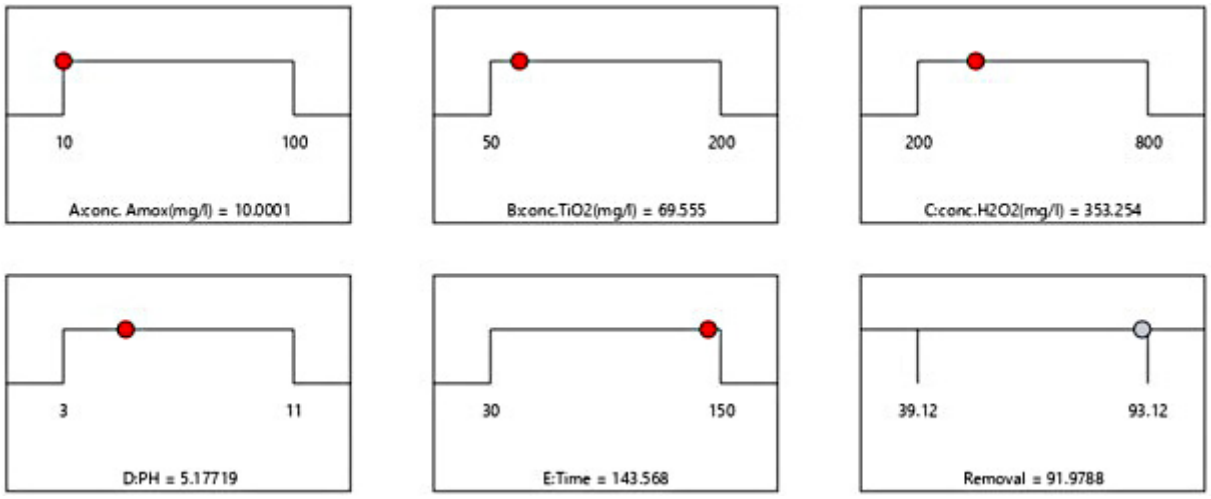

Fig. 9. Desirability profile of the predicted response

Table 6. Reaction rate constants in heterogeneous photocatalyst

First order		Second order	
K (min^{-1})	R^2	K (min^{-1})	R^2
0.0175	0.9198	0.0099	0.9862

residues removal from aqueous solution at pH = 5, H_2O_2 = 400 mg/l, and TiO_2/sand = 75 mg/l, and their results were shown in Table 6. The results revealed that the pseudo-kinematics of the second order showed the best correlation coefficient (R^2 = 0.95), and this is in agreement with the study of (Rahda and Ahmadi, 2018).

$$\ln \frac{C_o}{C} = k \quad (15)$$

$$\frac{1}{C} - \frac{1}{C_o} = kt \quad (16)$$

where: k is the reaction's rate constant, C and Co are the AMOX concentrations (mg/l) after exposure time t and the initial AMOX concentration (mg/l), respectively, and t is the exposure duration (min).

CONCLUSIONS

In the present study, RSM was used to optimize the effect of experimental factors on AMOX removal efficiency by using TiO_2 immobilized on sand in the presence of solar irradiation in photocatalyst process. The 3rd-order polynomial equation is used to build an empirical relationship between the response and independent variables based on experimental results. A high removal efficiency for AMOX was (91.9788%) was obtained at the optimum conditions (pH 5, catalyst TiO_2 / sand (69.555 mg/l), 10 mg/L of AMOX concentration, H_2O_2 concentration (353.254 mg/l) during 143.568 min), predicted by CCD have reasonable agreement with the value of 93.12% obtained by experimental work (pH 5, AMOX concentration of 10 mg/L, H_2O_2 concentration (400 mg/l), catalyst TiO_2 /sand = 75 mg/l during 150 min. ANOVA revealed a coefficient of determination (R^2 = 93.58%, R^2adj = 91.48% and R^2pred = 89.68%), indicating that the third regression model could be adjusted to the experimental data well. It's also worth noting that the photodegradation of AMOX appears to follow pseudo-second-order kinetics, with the rate constant being inversely proportional to the pollutant's initial concentration level.

Acknowledgements

The authors express their gratitude to the University of Baghdad (Baghdad, Iraq) for providing facilities for this research.

REFERENCES

1. Abdel-Maksoud Y.K., Imam E., Ramadan A.R. 2018. Sand supported TiO_2 photocatalyst in a tray photo-reactor for the removal of emerging contaminants in wastewater. Catalysis Today, 313, 55–62.
2. Balarak D., Mostafapour F., Joghtaei A. 2017. Thermodynamic analysis for adsorption of amoxicillin onto magnetic carbon nanotubes. British Journal of Pharmaceutical Research, 16(6), 1–11.
3. Bielan Z., Sulowska A., Dudziak S., Siuzdak K., Ryl J., Zielinska-Jurek A. 2020. Defective TiO_2 core-shell magnetic photocatalyst modified with

plasmonic nanoparticles for visible light-induced photocatalytic activity, Catalysts, 1–20(10), 672.

4. Chakrabarti S., Dutta B.K. 2004. Photocatalytic degradation of model textile dyes in wastewater using ZnO as semiconductor catalyst. J. Hazard. Mater, 112(3), 269–278.
5. Chauhan A., Sillu D., Agnihotri S. 2018. Removal of pharmaceutical contaminants in wastewater using nanomaterials: a comprehensive review. Current Drug Metabolism, 20(6), 483–505.
6. Chen F., Yang Q., Li X., Zeng G., Wang D., Niu C., Zhao J., An H., Xie T., Deng Y. 2017. Hierarchical Assembly of Graphene-Bridged Ag_3PO_4/Ag/$BiVO_4$ (040) Z-Scheme Photocatalyst: An Efficient, Sustainable and Heterogeneous Catalyst with Enhanced Visible -Light Photoactivity towards Tetracycline Degradation under Visible Light Irradiation, Applied Catalysis B: Environmental, 200, 330–342.
7. Daneshvar N., Salari D., Niaei A., Rasoulifard M.H., Khataee A.R. 2005. Immobilization of TiO_2 Nanopowder on Glass Beads for the Photocatalytic Decolorization of an Azo Dye C.I. Direct Red.Journal of Environmental Science and Health - Part A Toxic/Hazardous Substances and Environmental Engineering, 40(8), 1605–1617.
8. Danfá S., Martins R.C., Quina M.J., Gomes J. 2021. Supported TiO_2 in Ceramic Materials for the Photocatalytic Degradation of Contaminants of Emerging Concern in Liquid Effluents: A Review, Molecules, 26(17), 5363.
9. Darvishmotevalli M., Zarei A., Moradniac M., Noorisepehr M., Mohammadi H. 2019. Optimization of saline wastewater treatment using electrochemical oxidation process: Prediction by RSM method, Methods X, 6, 1101–1113.
10. Dutta S., Ghosh A., Moi M.C., Saha R. 2015. Application of Response Surface Methodology for Optimization of Reactive Azo Dye Degradation Process by Fenton's Oxidation. International Journal of Environmental Science and Development, 6(11), 818–823.
11. Elmolla E.S., Chaudhuri M. 2010. Photocatalytic Degradation of Amoxicillin, Ampicillin and Cloxacillin Antibiotics in Aqueous Solution using UV/TiO_2 and UV/H_2O_2/TiO_2 photocatalysis. DES, 252(1–3), 46–52.
12. Ghorbani F., Kamari S. 2017. Application of Response Surface Methodology for Optimization of Methyl Orange Adsorption by Fe-Grafting Sugar Beet Bagasse, Adsorption Science and Technology, 35(3–4): 317–338
13. Jouali A., Salhi A., Aguedach A., Lhadi E. 2020. Photo-Catalytic Degradation of Polyphenolic Tannins in Continuous-Flow Reactor using Titanium Dioxide Immobilized on a Cellulosic Material, Water Science & Technology, 82(7), 1454–1466.
14. Kalash K.R., Al-Furaiji M.H. 2020. Advanced Oxidation of Antibiotics Polluted Water using Titanium Dioxide in Solar Photocatalysis Reactor. Journal of Engineering, 26(2), 1–13.
15. Khataee A.R., Fathinia, M., Joo S.W. 2013. Simultaneous Monitoring of Photocatalysis of Three Pharmaceuticals by Immobilized TiO_2 Nanoparticles: Chemometric Assessment, Intermediates Identification and Ecotoxicological Evaluation. Spectrochimica Acta Part A: Molecular and Biomolecular Spectroscopy, 112, 33–45.
16. Kutuzova A., Dontsova T., Kwapinski W. 2021. Application of TiO2-Based Photocatalysts to Antibiotics Degradation: Cases of Sulfamethoxazole, Trimethoprim and Ciprofloxacin. Catalysts, 11(6), 728.
17. Lofranoa G., Pedrazzanib R., Libralatoc G., Carotenuto M. 2017. Advanced Oxidation Processes for Antibiotics Removal: A Review. Current Organic Chemistry, 21, 1–14.
18. Malakootian M., Nasiri A., Gharaghani M.A. 2019. Photocatalytic Degradation of Ciprofloxacin Antibiotic by TiO_2 Nanoparticles Immobilized on a Glass Plate, Chemical Engineering Communications, 207(1), 56–72.
19. Manassero A., Satuf M.L., Alfano O.M. 2017. Photocatalytic Degradation of an Emerging Pollutant by TiO_2-Coated Glass Rings: A Kinetic Study, Environmental Science and Pollution Research, 24(7), 6031–6039.
20. Méndez-López A., Zelaya-Ángel O., Toledano-Ayala M., Torres-Pacheco I., Pérez-Robles J.F., Acosta-Silva Y.J. 2020. The Influence of Annealing Temperature on the Structural and Optical Properties of ZrO_2 Thin Films and How Affects the Hydrophilicity. Crystals, 10(6), 454.
21. Mohammed A.A., Al-Musawi T.J., Kareem S.L., Zarrabi M., Al-Ma'abreh M. 2020a. Simultaneous Adsorption of Tetracycline, Amoxicillin, and Ciprofloxacin by Pistachio Shell Powder Coated with Zinc Oxide Nanoparticles. Arabian Journal of Chemistry, 13(3), 4629–4643.
22. Mohammed N.A., Alwared A.I., Salman M.S. 2020b. Photocatalytic Degradation of Reactive Yellow Dye in Wastewater using H_2O_2/TiO_2/UV Technique, Iraqi Journal of Chemical and Petroleum Engineering, 21(1), 15–21.
23. Morjène L., Tasbihi M., Schwarze M., Schomäcker R., Aloulou F.and Seffen M.2020. A Composite of Clay, Cement, and Wood as Natural Support Material for the Immobilization of Commercial Titania (P25, P90, PC500, C-TiO_2) towards Photocatalytic Phenol Degradation. Water Science and Technology, 81(9), 1882–1893.
24. Ngoepe N.M., Hato M.J., Modibane K.D., Hintsho-Mbita N.C. 2020, Biogenic Synthesis of Metal Oxide Nanoparticle Semiconductors for Wastewater

Treatment, Photocatalysts in Advanced Oxidation Processes for Wastewater Treatment.

25. Olama N., Dehghani M., Malakootian M. 2018. The Removal Of Amoxicillin From Aquatic Solutions Using the TiO_2/UV-C nanophotocatalytic method doped with trivalent iron. Applied Water Science, 8(4), 1–12.
26. Ozturk D., Sahan T., Bayram T., Erkus A. 2017. Application of Response Surface Methodology (RSM) to Optimize the Adsorption Conditions of Cationic Basic Yellow 2 onto Pumice Samples as a New Adsorbent. Fresenius Environmental Bulletin, 26(5), 3285–3292.
27. Salam K.K., Agarry S.E., Arinkoola A.O., Shoremekun I.O. 2015. Optimization of Operating Conditions Affecting Microbiologically Influenced Corrosion of Mild Steel Exposed to Crude Oil Environments Using Response Surface Methodology. British Biotechnology Journal, 7(2), 68–78.
28. Sharma K., Talwar S., Verma A.K., Choudhury D., Mansouri B. 2020. Innovative Approach of In-Situ Fixed Mode Dual Effect (photo-Fenton and photocatalysis) for Ofloxacin degradation. Korean J. Chem. Eng., 37(2), 350–357.
29. Tarfiei A., Services H., Eslami H., Ebrahimi A.A., Services H. 2018. Pharmaceutical Pollution in the Environment and Health Hazards, Journal of Environmental Health and Sustainable Development, 3(2), 491–495.
30. Tekin G., Ersöz G., Atalay S. 2018. Degradation of Benzoic Acid by Advanced Oxidation Processes in the Presence of Fe or Fe-TiO_2 Loaded Activated Carbon Derived from Walnut Shells: A Comparative Study. Journal of Environmental Chemical Engineering, 6(2), 1745–1759.
31. Tio N. 2017. Amoxicillin Photodegradation by Nanocrystalline TiO_2. Chemical Industry and Chemical Engineering Quarterly, 23(2), 187–195.
32. Tong K., Yang Y.L., Du X. 2020. Modelling of TiO_2-based packing bed photocatalytic reactor with raschig rings for phenol degradation by coupled CFD and DEM. Chemical Engineering Journal, 400, 125988.
33. Türkay G.K., Kumbur H. 2019. Investigation of Amoxicillin Removal from Aqueous Solution by Fenton and Photocatalytic Oxidation Processes. Kuwait J. Sci., 46(2), 85–93.
34. Zaier M., Vidal L., Garreau S.H., Balan L. 2017. Generating Highly Reflective and Conductive Metal Layers through A Light – Assisted Synthesis and Assembling of Silver Nanoparticles in A Polymer Matrix. Scientific Reports, 7, 1241.